FR8402929

22. International winter meeting on nuclear physics
Bormio (Italy) 23-27 Jan 1984
CEA-CONF--7247

Rapport DPh-N Saclay n° 2151 04/1984

EMISSION OF LIGHT FRAGMENTS IN HEAVY ION COLLISIONS DOES A LIQUID-GAS PHASE TRANSITION EXIST IN NUCLEAR MATTER ?

Y. CASSAGNOU

D.Ph.N/BE, CEN Saclay, 91191 Gif sur Yvette cedex, France.

EMISSION OF LIGHT FRAGMENTS IN HEAVY ION COLLISIONS DOES A LIQUID-GAS PHASE TRANSITION EXIST IN NUCLEAR MATTER ?

Y. CASSAGNOU

D.Ph.N/BE, CEN Saclay, 91191 Gif sur Yvette cedex, France.

Abstract

Fragments at large angle from a heavy ion collision could result from the condensation into clusters of nucleons from a hot zone of unbond nuclear matter. Analogy with the condensation of a vapour into droplets leads to predict a mass distribution of fragments of the form $\frac{d\sigma}{dA} \propto A^{-\tau}$ with $\tau \simeq 2.33$. In another proposed mechanism, nearly the whole ensemble projectile + target breaks into pieces due to the high excitation brought in by the collision. Then the charge distribution of fragments $\frac{d\sigma}{dZ} \propto \frac{1}{e^{1.28\frac{Z}{\sqrt{Z_o}}} - 1}$ is predicted.

Preliminary data from the reaction Ar + Au at 44 MeV/u are examined in the light of the two descriptions.

This talk will be devoted to the emission at large angles of light fragments which is often associated to the most violent heavy ion collisions i.e. those with small impact parameters. About this emission one has recently raised a very interesting theoretical question i.e. the possibility of a low energy phase transition in nuclear systems. Recent papers with titles like Nuclear Fragmentation [1] , Multifragmentation in nucleus-nucleus collisions [2] , Cold Break-up [3] , Nuclear Condensation [4] are equally related to the emission of light fragments.

I also will report on partial and preliminary data from an experiment which took place at Ganil last year when an ^{40}Ar beam of 44 MeV/u bombarded a target of Au. In this experiment, light particles from protons, deuterons, ... to ^{4}He particles were detected from 16° to 120° for energies up to 180 MeV. Light fragments, isotopically separated from ^{6}Li to ^{20}Ne, were also measured at angles between 17°5 and 85° with energies over 4 MeV/u. Even if one cannot hope for a clear understanding of the reaction mechanism to be derived from inclusive measurements the present data will be discussed in the light of a possible liquid-gas equilibrium. I am very grateful to Dalva CASTRO-RIZZO, Roland DAYRAS, Robert LEGRAIN, Louis RODRIGUEZ, Noëlle SAUNIER from Saclay, Roberto FONTE, Josette IMME-RACITI, Giovanni RACITI from Catania and Marie-Geneviève SAINT-LAURENT from Ganil who worked hard to make the data for the Ar + Au reaction at 44 MeV/u available.

I) Nuclear fragmentation and its large cross section.

In order to introduce the subject, let us look at figure 1 taken from a work of Jakobsson et al .... at CERN who irradiated emulsions with a ^{12}C beam of 70 MeV/u. In the analysis of the emulsion data two constraints were set : (1) the multiplicity (i.e. the number of tracks on fig. 1) should be higher than or equal to 11, (2) each track should correspond to a mass of the ionising nucleus lower than or equal to 11. If one makes a detailed balance of the number of nucleons playing a role in the event of fig. 1, one finds a total of 71 (4 d + 7 ^{3}He or ^{4}He + 3 ^{6}Li or ^{7}Li + 2 Be ions) which means, accounting for undetected neutrons, that a rather complete explosion of the target nucleus had occured (it would be a complete explosion if a Br nucleus of the emulsion was the target ; if it was a A_g nucleus, an additionnal, and not detected here, Z = 18 fragment should be added). The most striking result of these emulsion data comes from the statistics : events like that one in fig. 1 represents 20% of the total reaction cross section. Nuclear fragmentation is thus very important in heavy ion collisions.

The measurement of fragments emitted at large angle leads to the same conclusion. Fig. 2 gives, as an example, fragment cross sections as a function of their mass A (i.e. the mass distribution) from the reaction Ar + Au at 44 MeV/u. I apologize for showing these results prior to their derivation from the data. This will come later. We only consider here orders of magnitude : 40 barns for proton emission, 25 barns for d and α particles, 20 barns for t and ^{3}He. When these numbers are compared to the recently measured total reaction cross section of 4.8 barn [5] , one is lead to the conclusion that about 8 protons are emitted, as an average, per event. In the same way, we should have approximately 5 deuterons and 5 ^{4}He, 4 particles of mass 3, 1 fragment of Boron or Beryllium and finally 1 fragment of mass between 10 and 20. All these abundances confirm that most of the events we are interested in, as far as fragment emission is concerned, are of the explosion-type shown on fig. 1.

How can the large production of light nuclei in heavy ion collisions be explained ?

At the risk of giving a much restricted overview of recent theoretical developments , the list of which widely extends beyond the four previously quoted papers, we will consider only two different approaches to the problem.

II) Hot fragmentation.

The first one comes directly from high energy physics. It is the participant-spectator model in which the geometry of the reaction (size of the projectile, size of the target, range of possible impact parameters) defines average quantities, such as the number of participant nucleons, the volume, the temperature, from the overlap volume between the target and the projectile. This volume, eventually compressed if the projectile is heavy enough, receives all the energy available from the beam and form a sort of hot nuclear matter spot ; a small region of the target nucleus is excited to the point where nucleons act like free molecules of a gas, the state of which is entirely defined by a volume and a temperature.

Then this ensemble of free nucleons deexcite by transforming its thermal energy into kinetic energy in a process of expansion in all directions of space.

This is the point where the liquid-gas phase transition can take place. In the same way as a vapour condenses into droplets when its pressure decreases or its volume increases, the radial motion of expansion of the fireball could involve the "condensation" of fast nucleons into fragments.

Two conditions are required for a liquid-gas transition to be observed :

1) In analogy to the formation of droplets from an underpressurized vapour, the temperature, that is to say the excitation energy in the nuclear case, must be lower than a certain critical temperature. Too much energy would result, for the nuclear system, in permanently staying in the gazeous phase. The critical temperature was estimated from infinite nuclear matter calculations to lie between 8 and 13 MeV.

2) the second condition is a time-scale condition. A phase transition of first order can only be observed if the motion of expansion is slow enough for an equilibrium to settle at the time where the phase boundary is crossed.

Recent calculations from Bertsch at MSU [6] , Curtin Toki and Scott at the same place [7] , Stöcker [2] and Cugnon at Liège [8] show that these conditions could be met in heavy ion reactions below 100 MeV/u. The most favourable energies are predicted around 30-40 MeV/u. But this prediction rests upon calculations relative to infinite nuclear matter.

III) Cold fragmentation.

A second approach is the one of Aichelin, Huefner and Ibarra [3] . They start with a similar image of a fireball or a hot spot created by "participant" nucleons from the target and the projectile. The main difference from the previous description sets in when they essentially consider the fireball being trapped inside the cold spectator matter of the target. Only at the highiest energies, the possibility of some participants to escape at forward angles as fast nucleons is admitted, the projectile energy being then partly transferred to the target No clear-cut separation between "participants" and "spectators" seems to be implied by the model in any case.

Then the fireball deexcite in emitting fast nucleons in all directions through the surrounding cold target matter breaking it into pieces (fig. 3) . It is the image of the shattering of a sphere of glass which is shot down by a bullet and separates in parts according to preexisting weak bonds. In this view each fast nucleon from the fireball gives its momentum and energy to a more or less preexisting piece of the target. As fast nucleons are emitted from the fireball with equal probality in all directions, the production of fragments according to their size can be treated statistically.

Each fragment is furthermore accelerated by the repulsive Coulomb force from what remains of the target. This Coulomb repulsion is strongly dependent on the location where the fragment has been cut out from the target and which can be any place between the center and the surface. It is thus weighted by a distribution of all the possible distances from o to the target radius R.

The calculation of the fragment energies at a given angle depends on the distribution of impulsions received from the fireball nucleons, the initial F. .i .nomentum distribution of prefragments in the target, the additionnal impulsion gained from the weighted Coulomb repulsion and lastly the contributive impulsion from the trapping of the initial fireball in the target.

This approach was named by its authors "cold break-up". In contrast to the thermal approach, it is a two-step process (fireball formation, knock-on of fragments)in which each step is a fast one. It refers to a non-equilibrated process. As a consequence, there is no hope for an equilibrium, of a liquid-gas type for example, to set up.

IV) Experimental angular distributions of fragments.

Let us now have a look on the data. We will first consider the fragments which are easier to understand and then the light particles. Fig. 4 shows energy spectra of ^{6}Li ions emitted at various angles from 32°5 to 77°5 in the reaction ^{40}Ar + Au at 44 MeV/u. The upper curve is for the smallest angle, the lower curve for the largest angle. Counts on the vertical axis are on a logarithmic scale. Two features are prominent on the figure :

1) The high energy part of the spectrum shows a slope which becomes steeper with increasing angle.

2) There is a maximum in the spectrum in the low energy part and this maximum is moving to lower energies with increasing angle.

This shape i.e. the maximum, the constant slope and their angular dependance are well known from thermodynamics to be typical of an emission of particles from a moving source.

One has got used to represent these spectra on a velocity plot with $\beta_{//}$ on the horizontal axis and $\beta_{\perp}$ on the vertical one. One calculates invariant cross ssections which are represented by contour lines. If relativistic corrections can be neglected, cross sections measured at a definite lab angle give points on a straight line starting from the origin of coordinates.

Fig. 5 shows such a plot of velocity spectra for the invariant cross sections derived from the data of fig. 4. One can see a ridge which would actually be crescent-shaped if the forward angles could have been reported to show the complete pattern. The forward angles were on purpose removed here since other mechanisms contribute at these angles ; for example, the fragmentation of the projectile gives a high energy component starting at $\beta = 0.3$, the velocity of the projectile. There is also a low energy component from the symetric process

of target fragmentation. Because of this filling of the low and high energy part of the spectrum, the ridge at intermediate energy becomes difficult to spot.

To explain fig. 5 by the emission of a moving source, we used the following expression :

$$\frac{d\sigma}{d\Omega\, dE} = cst \,.\, \sqrt{E - ZE_c} \,.\, e^{-(E - ZE_c + E_s - 2\sqrt{E_s}\sqrt{E - ZE_c}\cos\theta)/T}$$

in which $\beta_s = \frac{V_s}{c}$ is the velocity of the source, $E_s = \frac{1}{2}\, m\, V_s^2$ its energy per nucleon (of mass m) and T its temperature.

This expression can be derived easily from the classical distribution of impulsions from a moving source :

$$\frac{d^6 n}{d^3 r\, d^3 p} \propto e^{-(\vec{p} - \vec{p}_s)^2 / 2m\, KT} \qquad \text{(K = Boltzmann constant)}$$

which becomes in the form of the measured cross sections

$$\frac{d\sigma}{d\Omega\, dE} \propto p.e^{-(\vec{p} - \vec{p}_s)^2 / T}$$

or

$$\frac{d\sigma}{d\Omega\, dE} \propto \sqrt{E}.e^{-(E + E_s - 2\sqrt{E}\sqrt{E_s}\cos\theta)/T}$$

In the case of charged particles, the Coulomb force exerts itself between the fragment and the remainder of the target. This has the consequence of accelerating the fragment, so its kinetic energy in the above expression has to be reduced. This is achieved by replacing E by $E - ZE_c$ with Z being the charge of the fragment and E_c the amplitude of the Coulomb correction. Then expression (1) is obtained.

Fig. 6 shows the contour line pattern obtained with equation (1) with the following parameters for the moving source : $\beta_s = 0.1$ i.e. approximately 1/3 of the target velocity while the compound nucleus velocity would be 0.05. The temperature T is 16 MeV and the Coulomb correction, 5 MeV per charge, represents nearly half the Coulomb barrier for two touching spheres. If one remembers the previous argument in connection with the Aichelin model about the fragment being formed at any place between the center and the surface of the target nucleus, this low value of the Coulomb repulsion is easily understood.

All fragments between mass 6 and 15 were fitted with rather similar values for the three parameters β_s, T, E_c as is shown on fig. 7. however, the source velocity β_s was found averaging a somewhat lower value of 0.8 for fragments of mass greater than 6.

Fig. 8 shows the cross sections at different angles in the lab frame for ^{11}B fragments along with those calculated using equation (1) and the set of parameters (β_s = 0.08, T = 16 MeV, E_c = 5 MeV) which fitted almost the whole fragment production. Here the data at forward angles (17°5 and 25°) are reported. One can easily see at these angles the large compcnent at high energy due to the projectile fragmentation which is not fitted by the calculated curves. At backward angles, the fit is only fair. This is so because in the fitting procedure, the same weight was given to each data point. Cross sections at backward angles become rapidly small and energy spectra are made up with a few points in contrast to forward angles. Thus at backward angles the fit is poorer. Nevertheless, the agreement of fig. 8 should be considered as more meaningful than a simple parametrization since it corresponds to a severe constraint on many angles and on a large energy domain and furthermore, the angular distribution of more than a dozen of fragments have been well reproduced with the same set of parameters and with equal quality in the fit.

V) Angular distributions of light particles.

Let us now look at the light particles. Fig. 9 shows the velocity plot associated with the protons in the ^{40}Ar + Au reaction. The dotted contour lines represent calculations with equation (1) while the solid lines are the experimental invariant cross section. No satisfactory fit could be obtained. By slightly modifying β_s and decreasing T_s down to 10 MeV as was done with fig. 9, the χ^2 is still more than an order of magnitude larger than in the previous fits to the fragments. Clearly, we have on fig. 9 a large contribution from high energy protons due to the projectile fragmentation even at intermediate angles and also low energy protons are coming from the target at backward angles. The deuterons and, to a less extent, theα particles show the same features as the protons. A calculation with three emitting sources with projectile velocity, target velocity and intermediate velocity, failed to reproduce the pattern of fig. 9. Obviously, the protons and to a lesser extent other light particles are less selective to the reaction mechanisms or impact parameters than heavy fragments. Also the source cannot possibly be considered punctal any more but has to be given a width in space and in velocity. Only by triggering on the multiplicity of associated charged (light) particles, one could hope to get the same information as given by the fragments.

VI) Equation of state - Calculations

Let us come back to the fragments once more.

Integrating the spectra at various angles of fig. 8 over the particle energy, an angular distribution is obtained, as that shown on fig. 10 for ^{18}O fragments. ^{18}O was selected because it is not, by far, the most abundant detected fragment and still the

main feature of all these angular distributions is clearly seen : an exponential decrease with lab angle. Up to now the significance of this shape is unclear. We only used it as a pratical way of parametrization in order to calculate the total fragment yields. The dependance on A or Z of these yields will now be discussed and compared to the predictions of the two theoretical approaches which were described above.

Now, let us come back to the liquid-gas equilibrium problem, and previously to this simple remark : we have succeeded in fitting velocity plots of the fragments from ^{6}Li to ^{20}Ne in the Ar + Au reaction by a parametrization based on the motion of an emitting source (eq. 1). Let us take it more seriously and consider that the fit gives evidence for the formation of a fireball of velocity $\beta \simeq 0.1$ i.e. 1/3 of the velocity of the projectile. If one uses the approximate formula given by Swiatecki to estimate the most probable number of nucleons from the projectile which can be found as "participants" in the fireball, one gets 30. If the fireball velocity is O.1, it means that 60 more nucleons from the target "participates" in the fireball. Now, the 30 incident nucleons have a kinetic energy of 30 x 44 = 1320 MeV and bring in the fireball a C.M. energy $1320 \times \frac{60}{90} = 880$ MeV. This is the excitation energy given to 90 nucleons. So each one get 10 MeV on average. Clearly, there is a large probality for the fireball to be made of unbound nuclear matter.

Actually, this is the basic assumption of all the calculations where a few nucleons receive the largest fraction of the beam energy (hot spot, fireball ...). Fig. 11 shows, as an example, a plot of the pressure versus density which can be derived from the equation of state of hot nuclear matter. The figure shows that if the temperature of a nuclear system is lower than 20 MeV (the "critical temperature") a region of coexistence between a liquid phase and a gazeous phase can exist. This appears as a consequence of the shape of the equation of state which can be written in a way similar to the Van der Waals equation for a fluid. Actually, the expansion of the fireball is not described by isotherms such as those indicated on fig.11 but rather by iso-entropic (equal entropy) curves which cross isotherms of decreasing temperature. This leads to diagram such as that of fig. 12 [8] . Solid curves represent the evolution of a hot nuclear system starting from a point located in the upper and right part of the figure ($\rho \geqslant 0.15$ fm $^{-3}$). If the excitation of the fireball (i.e. temperature) is too high so that the initial entropy of the system is greater than 2, the evolution of the state is smooth as would be the case for a system kept permanently in the gazeous phase. If the initial entropy is lower than 2, let us say for example S = 1, the expansion can lead the system into the region of density $\rho = 0.05$ in an instable state where the derivative of the pressure against density is negative. In such a case, the system is predicted to condense into fragments in a complete analogy with a vapour which condenses into droplets.

VII) Condensation Theory

The condensation theory is a recent work (Fisher , 1967) [9] which predicts the size A of droplets from a condensed vapour to be given by the following distribution :

$$P(A) = A^{-\tau} \cdot e^{-(a A^{2/3} + b A - \mu A)/T} \qquad (2)$$

where a = a (T) is the surface free energy per particle, b = b (T) is the volume free energy per particle and μ is the chemical potential per particle. If x and y are two quantities defined as follows :

$$x = e^{-a/T}$$

$$y = e^{-(b-\mu)/T}$$

then the Fisher law can be rewritten as :

$$P(A) = A^{-\tau} \, x^{A^{2/3}} \, . \, y^{A}$$

In the vicinity of the critical point, it can be shown that, if $T \gg T_c$, the surface energy is zero since the droplets disappear into vapour and, if $T \leqslant T_c$, the volume energy is equal to the chemical energy because the Gibbs free energy per particle is zero.

Then for $T \simeq T_c$, the quantities $x \simeq y \simeq 1$ and the distribution (2) has the simple form :

$$P(A) = A^{-\tau} \qquad (3)$$

For a Van der Waals gas, τ should be 7/3 . For real gases, values of τ were measured ranging between 2 and 3 with the most probable value not far from 2.33 i.e. the Van der Waals gas value [10] .

In analogy with real gas theory , the nuclear condensation picture predicts a maximum in fragment production at the critical temperature. As the fragment mass distribution is given by equation (3) about this point, one should observe a minimum of τ as a function of energy (or temperature). The existence of this minimum would bear evidence for a liquid-gas equilibrium.

VIII) Fragment mass distributions. Experimental and calculated.

The mass yields of fragments from a set of proton-induced and heavy ion-induced reactions at intermediate and high energies have recently been analyzed with the help of equation (2)[or equation (3) valid in the vicinity of the critical temperature]. Fig. 13 gives an example in which the value of the exponent τ results from a fit to the mass distribution with equation (3).

A "temperature" has also been derived from rapidity or velocity plots in the same way as the one we used for the data of fig. 6. In some cases, the temperature is simply a slope parameter derived from energy spectra.

When τ is plotted versus the "temperature", fig. 14 is obtained. Lots of criticism was hurlded at this figure since several systems are invoked with no garantee of the independence between temperature and system. Despite this objection, the variation of τ versus "temperature" (fig. 14) indicates the possibility of a minimum of τ around 11 MeV [11] very close to the predictions quoted above. Honesty obliges to say that the same data, or nearly the same, has been read in a way leading to quite the opposite conclusion : the dependence of τ versus energy is smooth and this rules out any evidence for a liquid-gas equilibrium [12] . The truth is that present data are not conclusive enough !

The yields of fragments from the reaction ^{40}Ar + Au at 44 MeV/u are shown on fig. 15 and compared to a distribution of the form $Y(A) = A^{-\tau}$. A reasonnable fit is obtained with $\tau = 2.33$. But the present data cannot be considered as giving evidence for condensation phenomena. Indeed, as it can be seen on fig. 13 and 15, nuclear structure effects induce fluctuations in the yields of light masses (A<10). For example, a lowering of A = 6 and A = 9 cross sections shows up due to the small binding energies of ^{6}Li and ^{8}Be. Consequently the ^{4}He and d yields should be increased. The significant data is then limited to the small region of masses between 10 and 20 on fig. 15. Mass A = 24 and 27 yields show a sudden decrease which reflects poor efficiency in detecting these isotopes due to the thickness of the first ΔE element of the telescopes.

We hope that more accurate and extensive data in the region $20 < A < 40$ from a new experiment would help to determine τ with confidence in this ^{40}Ar + Au reaction. Moreover τ should be known for the same system at different energies to obtain valid information about the possible existence of a low energy transition phase.

The 44 MeV/u ^{40}Ar + Au yield distribution has been compared to the predictions of the cold break-up model of Aichelin et al .... [3] on fig. 16. Here cross-sections are summed over the fragment charge Z since the predicted yield distribution has the form [13] :

$$Y(Z) = \sigma_F \cdot \frac{1}{e^{1.28 \frac{Z}{\sqrt{Z_o}}} - 1} \qquad (4)$$

In this relation, σ_F is the total fragmentation cross section and Z_o is the charge of the nuclear system the fragments of which are detected. If Z_p and Z_T are the projectile and target charges respectively, Z_o should be :

$$Z_o = Z_p + Z_T - Z_{fast}$$

which express the assumption that the "participant" nucleons of the initial hot zone (fireball or hot spot) remain inside the cold "spectator" matter, with the exception of a few fast nucleons (Z_{fast}) escaping at the very forward angles.

Equation (4) results straightforwardly from the conservation of charge and the principle of minimal information or maximal entropy. Thus, no specific mechanism is assumed in the Aichelin et al ... model and the charge distribution is considered as independent of energy and angle distributions (experiment agrees somewhat with this), so that all possible fragmentation modes of the total available charge Z_o have probabilities governed only by statistics.

Fig. 16 shows an agreement between experiment and calculation which is not so good as on fig. 15 yet not so bad as to reject it. As for the previous model, present data do not look accurate enough to support any definitive conclusion.

We tried various values of Z_o, the only adjustable parameter in equation (4). In a reaction such as ^{40}Ar + Au, Z_o is large resulting in a distribution (4) rather insensitive to sensible changes in Z_o. Actually a good fit to the experimental data is obtained only with very small values of Z_o which have no physical significance. Conversely, on can hope that more accurate data will yield a stringent test of this model.

REFERENCES

1 G. Bertsch and P.J. Siemens, Phys. Lett. 126B, 9, (1983)

2 H. Stöcker et al ...., Nucl. Phys. A400, 63c, (1983)

3 J. Aichelin, J. Huefner, R. Ibarra, peprint Univ. of Heidelberg (Germany), (1983)

4 H. Jaqaman, A.Z. Mekjian, L. Zamick, Phys. Rev. C27, 2782, (1983)

5 N.Alamanos et al ..., Phys. Lett. 137B, 37,(1984)

6 G.F. Bertsch, Nucl. Phys. A400, 221c, (1983)

7 M.W. Curtin, H. Toki, D.K. Scott, Phys. Lett. 123B, 289, (1983)

8 J.Cugnon, Phys. Lett. 135B, 374, (1984)

9 M. Fisher, Physics Vol. 3, 255, (1967)

10 C.S. Kiang, Phys. Rev. Lett. 24, 47, (1970)

11 A.D. Panagiotou, M.W. Curtin, H. Toki, D.K. Scott, P.J. Siemens
M.S.U. Report MSUCL 433, (sept. 1983)

12 D.H. Boal, M.S.U. Report MSUCL 443, (Dec. 1983)

13 J. Aichelin and J. Huefner, Phys. Lett. 136B, 15, (1984)

14 B. Jakobsson et al..,Z.Physik A307, 293, (1982)

15 A.S.Hirsch et al ..., Phys. Rev. C29, 508, (1984)

FIGURE CAPTIONS

Fig. 1 - ^{12}C (70 MeV/u) + Ag Br. Explosion - type events (multiplicity $M \geqslant 11$ of fragments $A \leqslant 11$) represent 20 % of σ_R [14] .

Fig. 2 - ^{40}Ar (44 MeV/u) + Au. Fragment yields.

Fig. 3 - Oblique - hatched zone : fireball region where beam energy and momentum is deposited ; cross - hatched zone : fragments cut out in the cold spectator by fast nucleons from the fireball [3] .

Fig. 4 - ^{40}Ar (44 MeV/u) + Au Energy spectra of ^{6}Li ions.

Fig. 5 - ^{40}Ar (44 MeV/u) + Au $\longrightarrow$ ^{6}Li + ... Velocity plot. Experimental.

Fig. 6 - ^{40}Ar (44 MeV/u) + Au $\longrightarrow$ ^{6}Li + ... Velocity plot calculated with a moving source of velocity β_S and temperature T. E_c is the Coulomb correction per charge on the fragment energy E.

Fig. 7 - ^{40}Ar (44 MeV/u) + Au $\longrightarrow$ ^{8}B + ... Angular distributions. Experimental (dots) and calculated (full lines) with the moving source parametrization

Fig. 8 - Dependence of the moving source parameters on fragment mass A.

Fig. 9 - ^{40}Ar (44 MeV/u) + Au $\longrightarrow$ p + ... Velocity plot. Experimental and calculated (one moving source).

Fig.10 - ^{40}Ar (44 MeV/u) + Au $\longrightarrow$ ^{18}O + ... Angular distribution.

Fig. 11 - Pressure - density plot for infinite nuclear matter. T_c = 20 MeV = critical temperature. $\rho_c \simeq 0.4\ \rho_o$. Isotherm T = 15 MeV shows up a region of negative compressibility which corresponds to a phase transition between liquid and gas [7] .

Fig. 12 - Pressure - density plot for infinite nuclear matter. The fireball evolution is represented by iso - entropes (plain curves) crossing isotherms (dashed curves) of decreasing temperatures. For entropy $S < 2$ a region of negative compressibility appears around $\rho = 0.3\ \rho_o$, favourable for a liquid - gas equilibrium to settle [8] .

Fig. 13 - $p + Xe \longrightarrow A_f + X$ [80 GeV < E_p < 300 GeV] . Fragment mass yields [15] .

Fig. 14 - Plot of exponent τ versus "temperature". Data from various proton- induced and heavy ion induced reactions.

Fig. 15 - ^{40}Ar (44 MeV/u) + Au. Fragment mass yields. $A^{-\tau}$ law is fitted on experimental points except A = 6 and 8 (nuclear structure effects are responsible for the low cross sections of there two masses).

Fig. 16 - ^{40}Ar (44 MeV/u) Fragment mass yields and the prediction of the Aichelin et al .... model [13] .

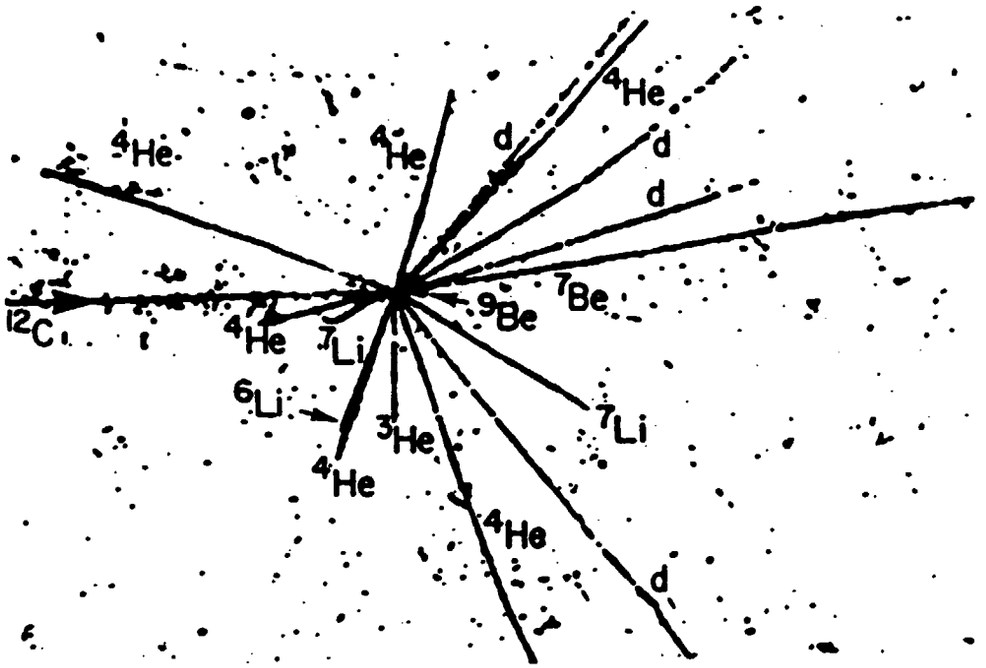
4He
4He
4He
d
d
d
12C
4He
7Li
6Li
3He
4He
9Be
7Be
7Li
4He
d

Fig 1

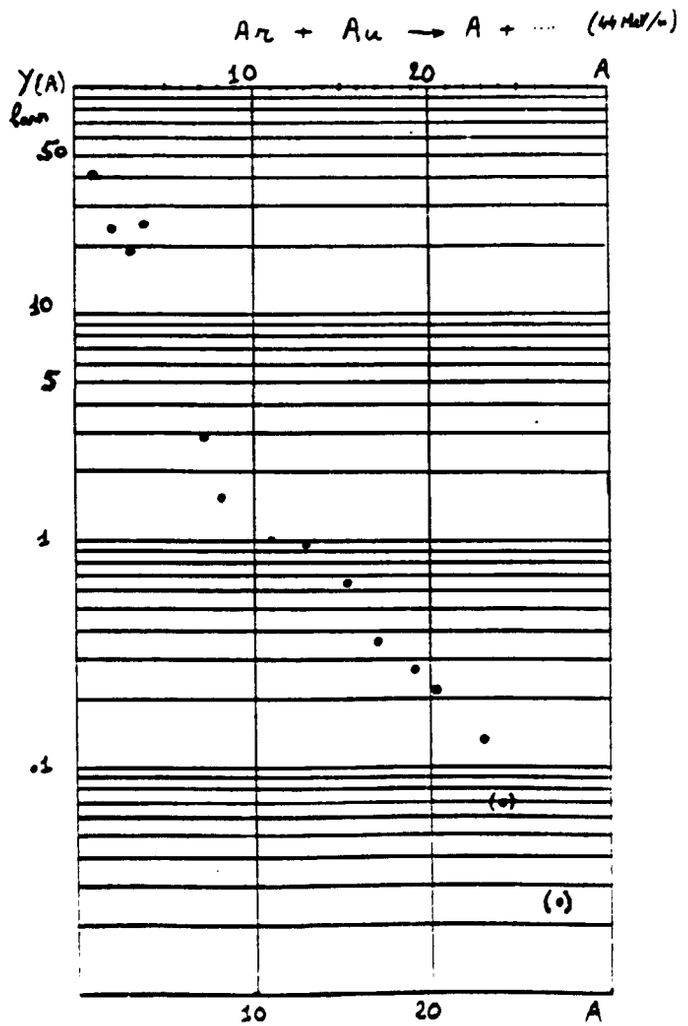
Ar + Au → A + ···· (44 MeV/u)
Y(A)
barn
50
10
5
1
.1
10
20
A
10
20
A

Fig 2

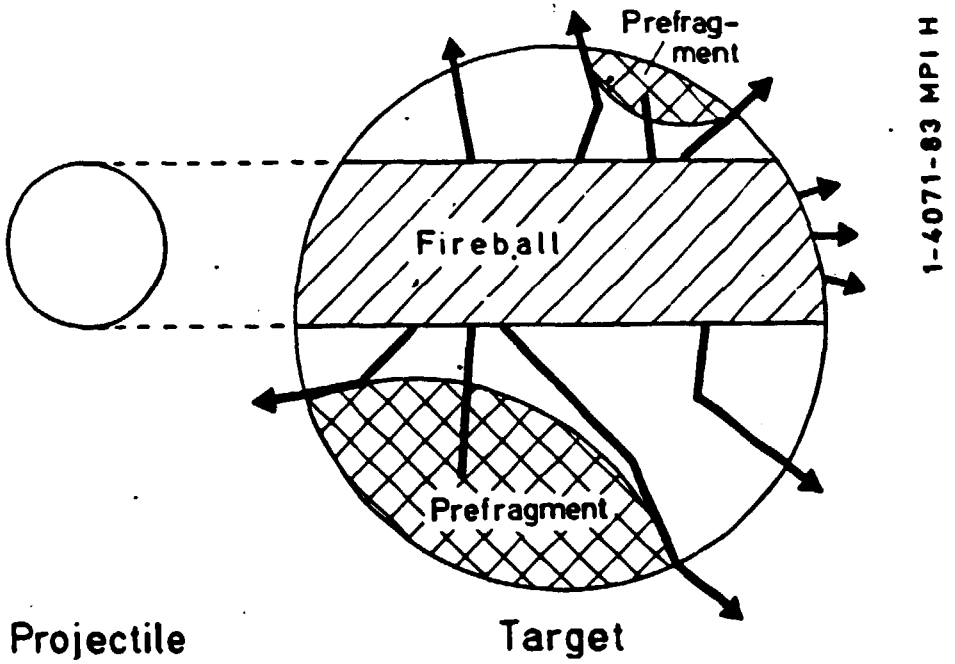
Prefrag-
ment
Fireball
Prefragment
Projectile
Target
1-4071-83 MPI H

Fig 3

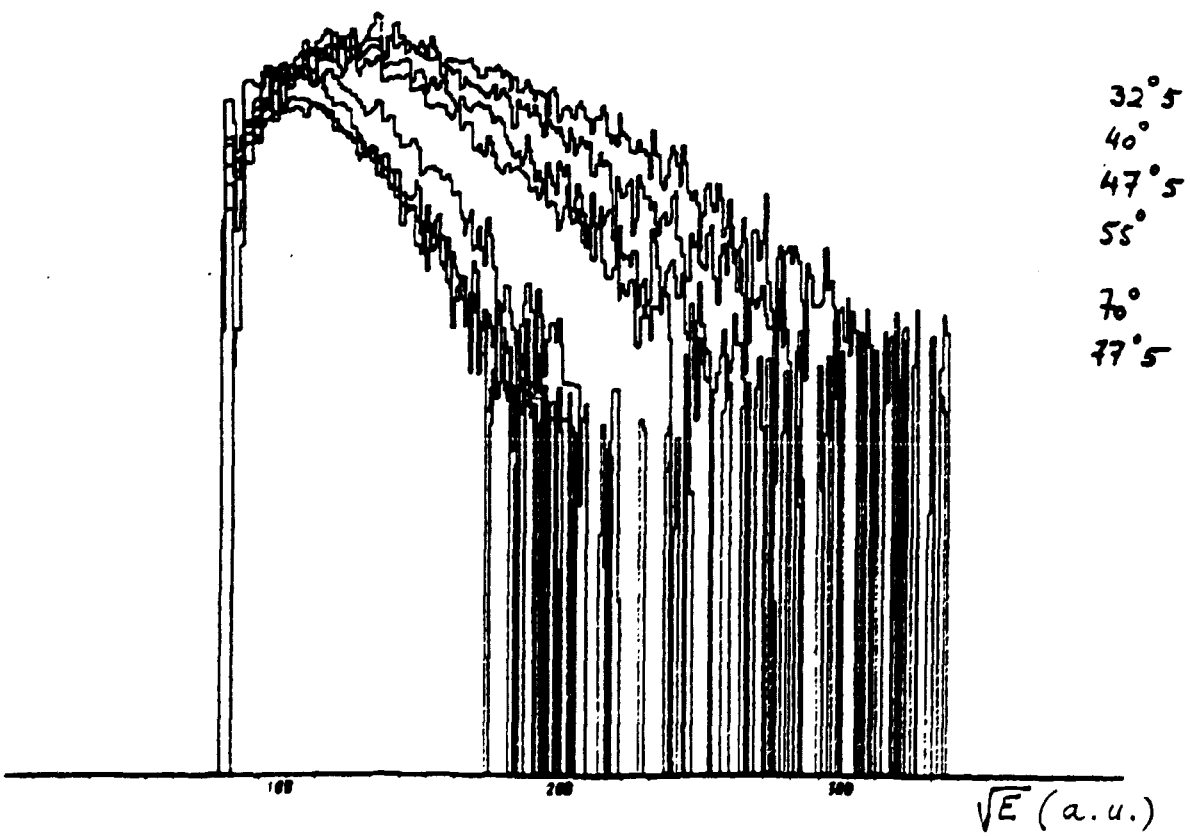
32°5
40°
47°5
55°
70°
77°5
100
200
300
√E (a.u.)

Fig 4

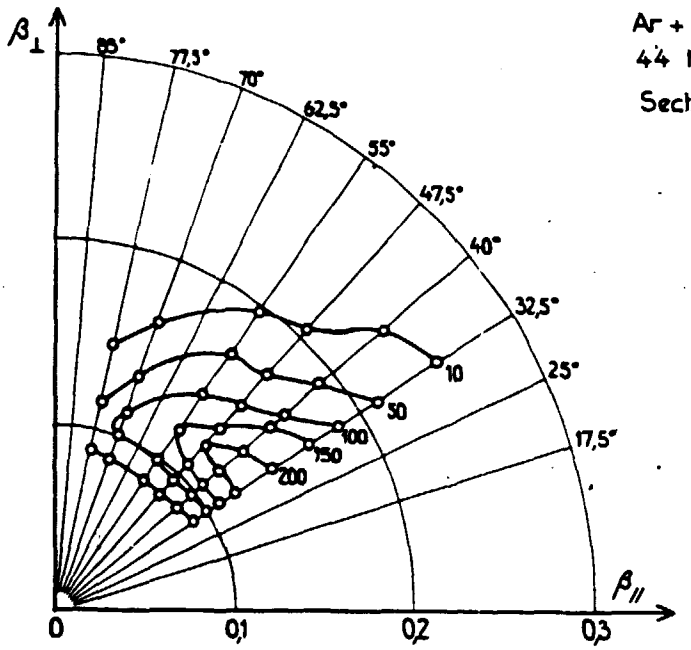

$Ar + Au \rightarrow {}^{6}Li + \ldots\ldots$
44 MeV / u
Sect. eff. en $\frac{nb/Sr}{(MeV/c)^2}$

Fig 5

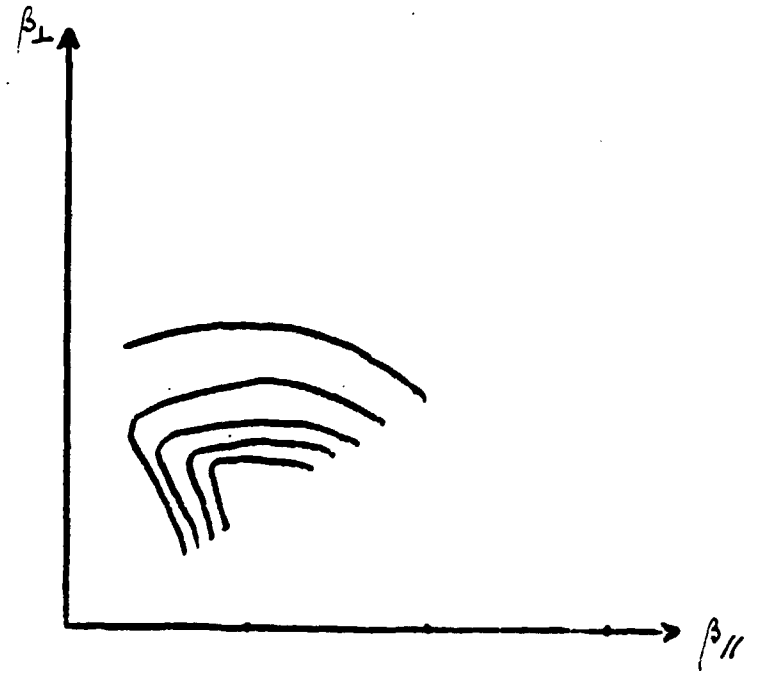

$\beta_s \approx 0.11$
$T \approx 16$ MeV
$E_c = 5$ MeV

$$\frac{d^2\sigma}{d\Omega\, dE} = C^{ste} \times \sqrt{E - 2E_c}\; e^{-\left(E - 2E_c + E_s - 2\sqrt{E_s}\sqrt{E-2E_c}\cos\theta\right)/T}$$

Fig 6

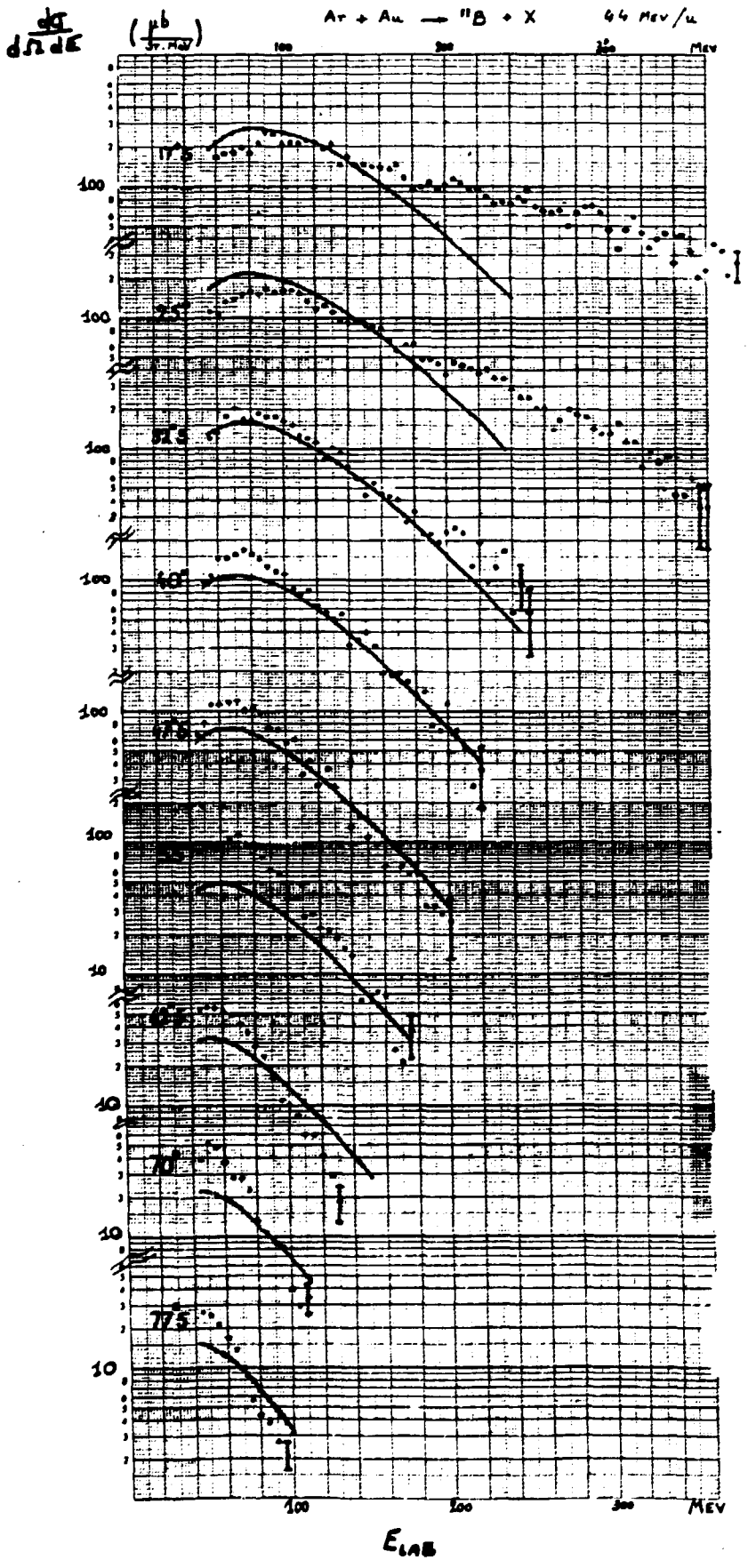
Ar + Au → ¹¹B + X
44 MeV/u
dσ/dΩdE (μb/sr.MeV)
17.5°
25°
32.5°
40°
47.5°
55°
62.5°
70°
77.5°
100
200
300
MeV
E_LAB

Fig 7

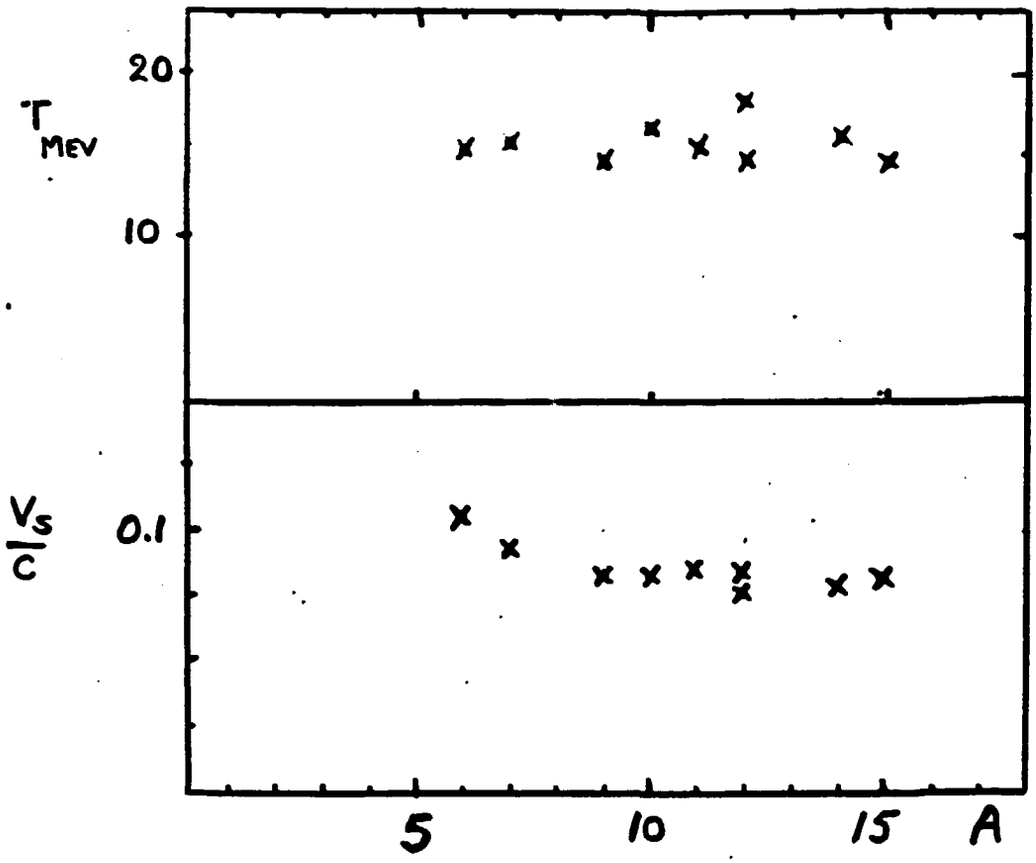
20
T_{MEV}
10
$\frac{V_s}{c}$
0.1
5
10
15
A

Fig 8

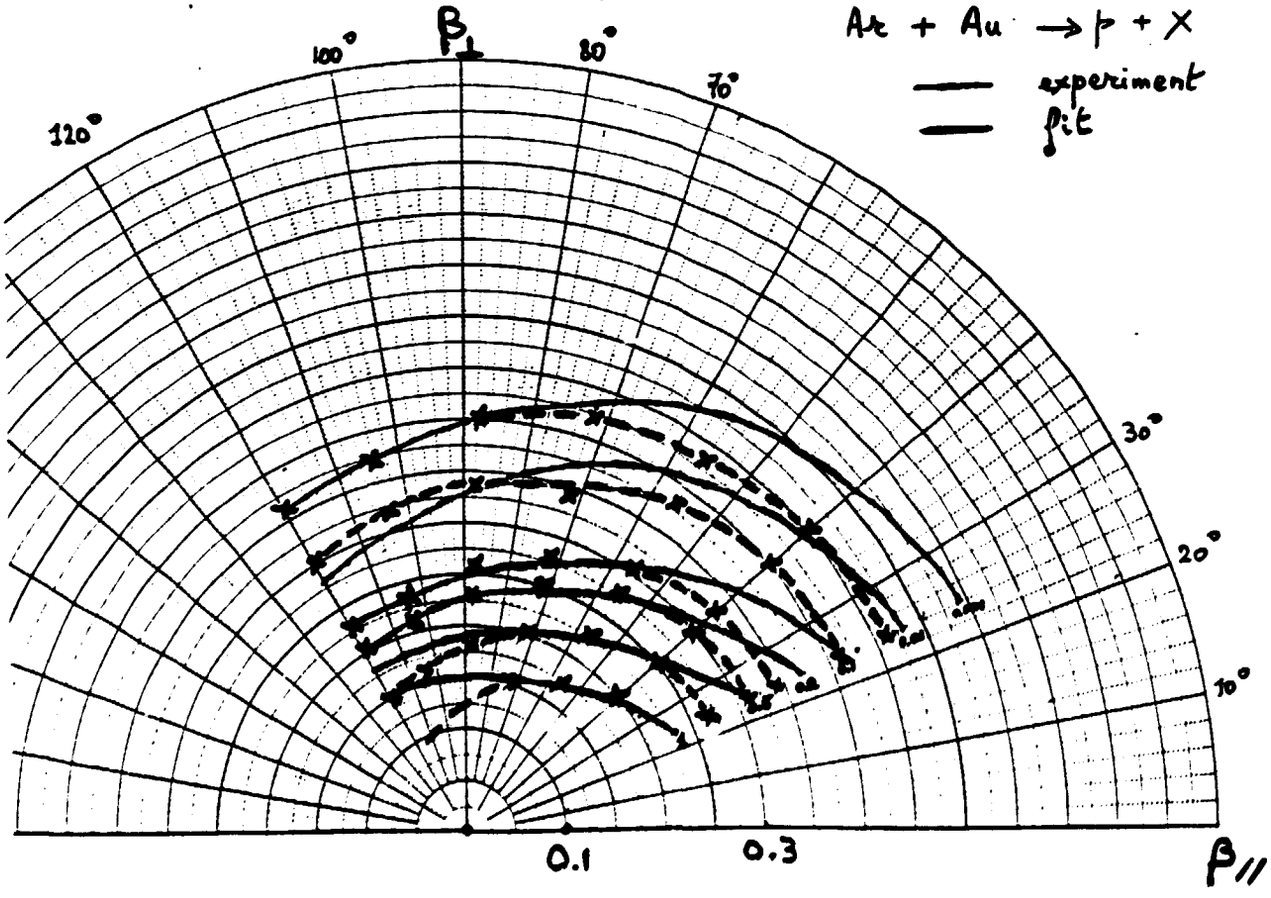
$\beta_\perp$
100°
80°
70°
120°
Ar + Au → p + X
experiment
fit
30°
20°
10°
0.1
0.3
$\beta_{//}$

Fig 9

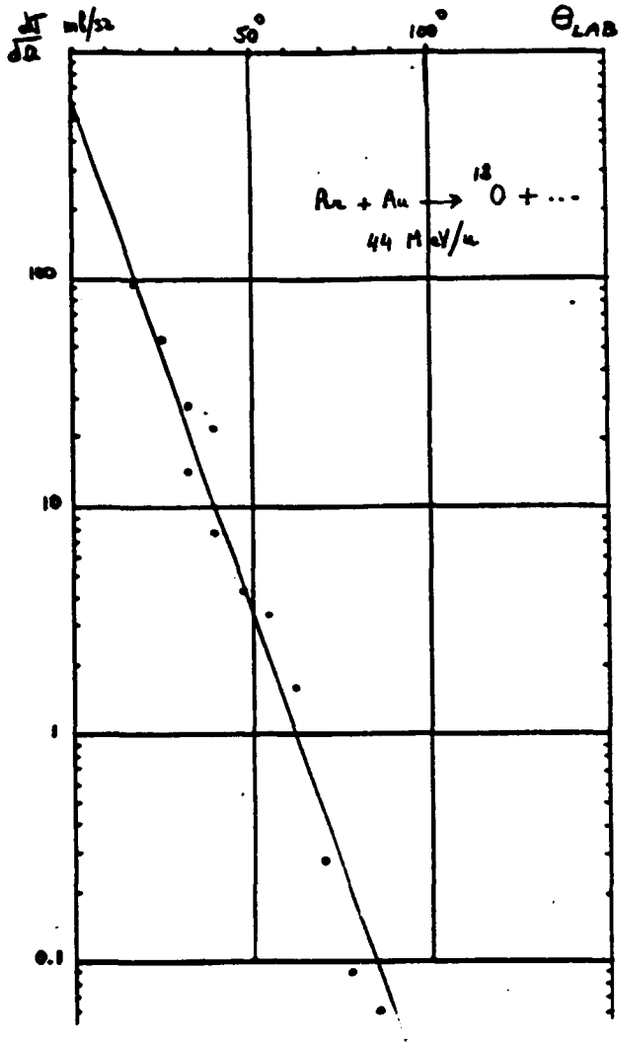
50°
100°
θ_{LAB}
Ne + Au → ^{18}O + ...
44 MeV/u
100
10
1
0.1

Fig 10.

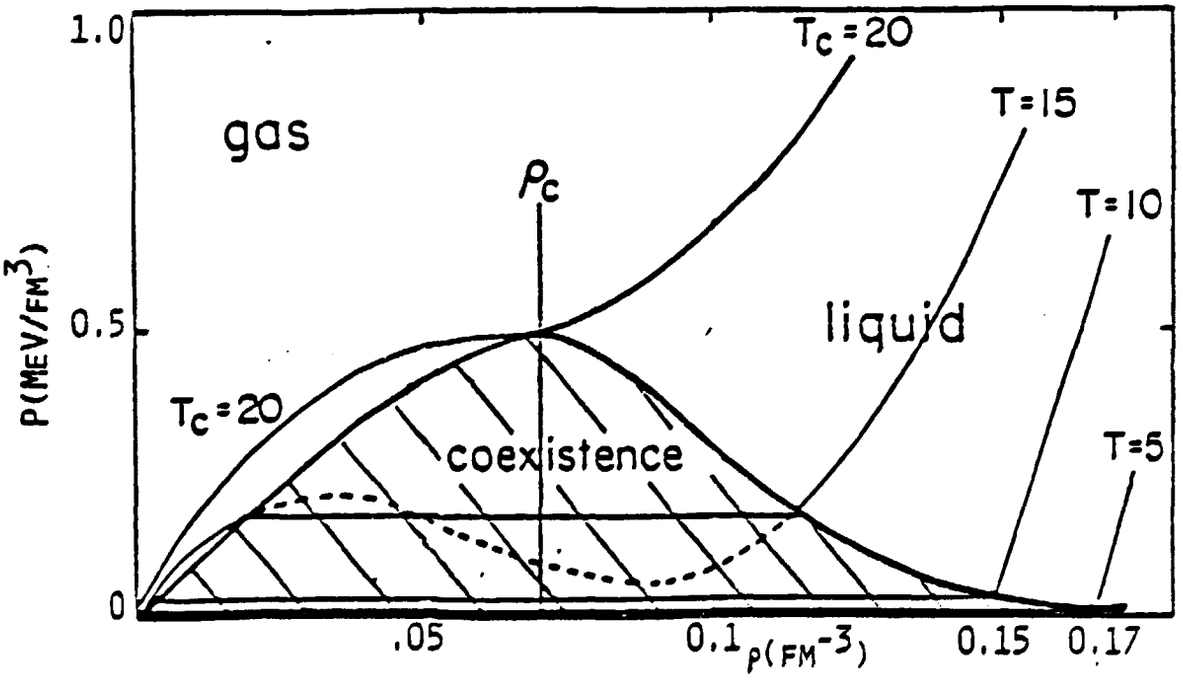
1.0
0.5
0
P(MEV/FM^3)
gas
liquid
coexistence
ρ_c
T_c=20
T=15
T=10
T=5
T_c=20
.05
0.1
ρ(FM^{-3})
0.15
0.17

Fig 11

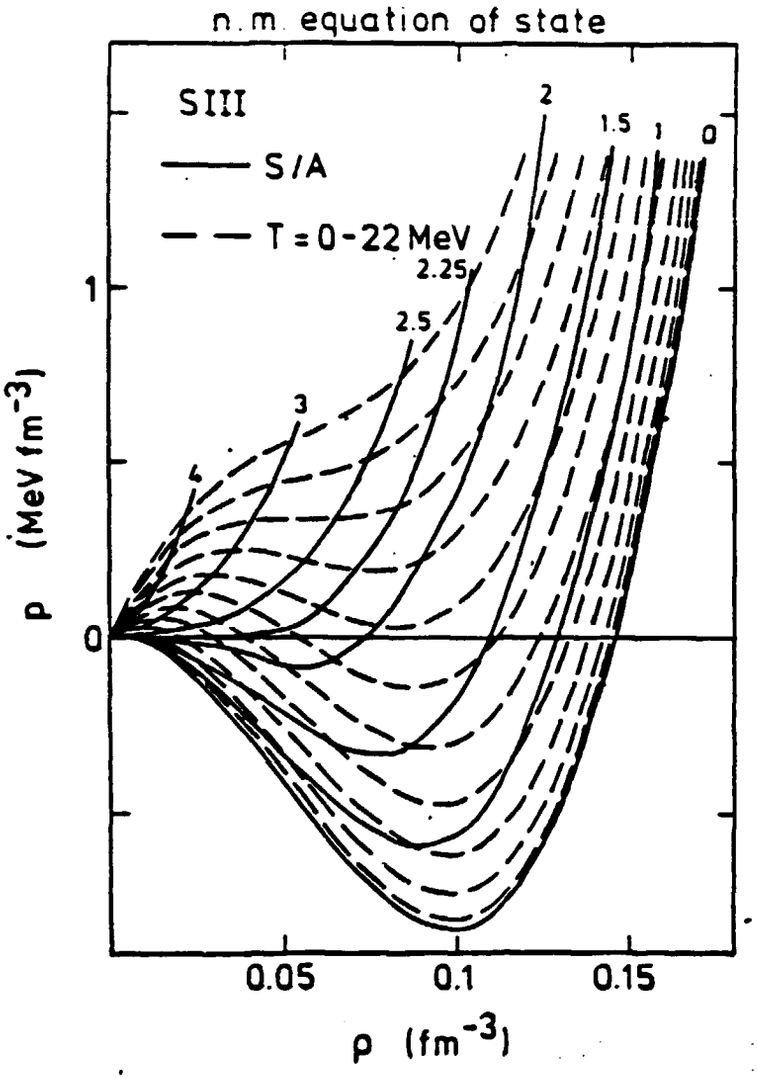
n.m. equation of state
SIII
S/A
T = 0-22 MeV
2
1.5
1
0
2.25
2.5
3
4
1
0
p (MeV fm^{-3})
0.05
0.1
0.15
ρ (fm^{-3})

Fig 12

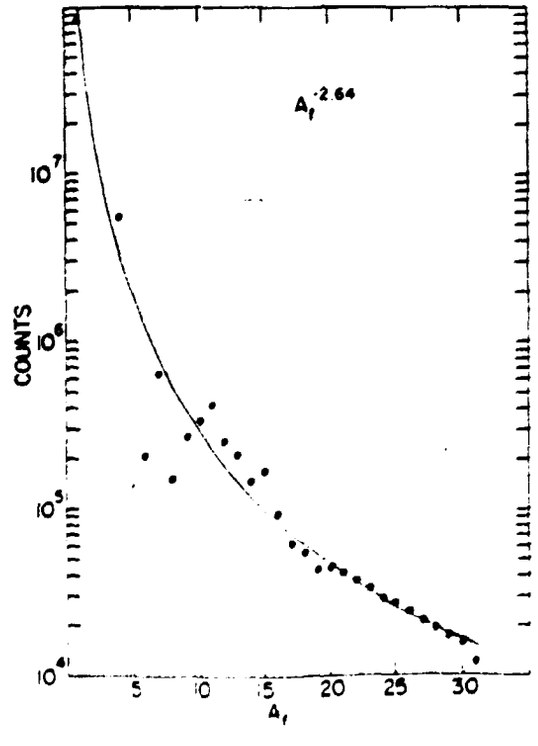
$A_f^{-2.64}$
10^7
10^6
10^5
10^4
COUNTS
5
10
15
20
25
30
A_f

Fig 13

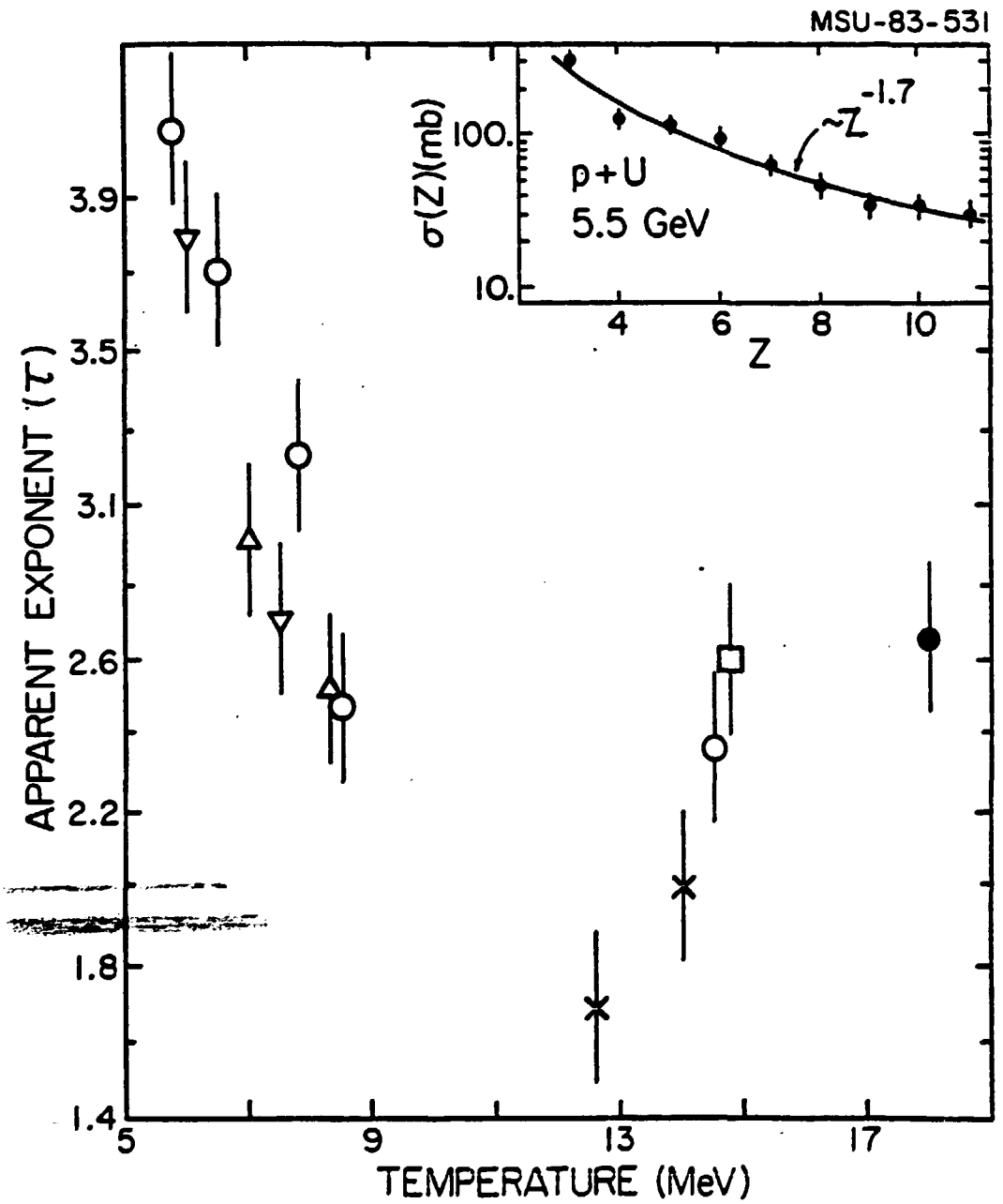
MSU-83-531
APPARENT EXPONENT (τ)
TEMPERATURE (MeV)
3.9
3.5
3.1
2.6
2.2
1.8
1.4
5
9
13
17
σ(Z)(mb)
100.
10.
p+U
5.5 GeV
~Z^-1.7
4
6
8
10
Z

Fig 14

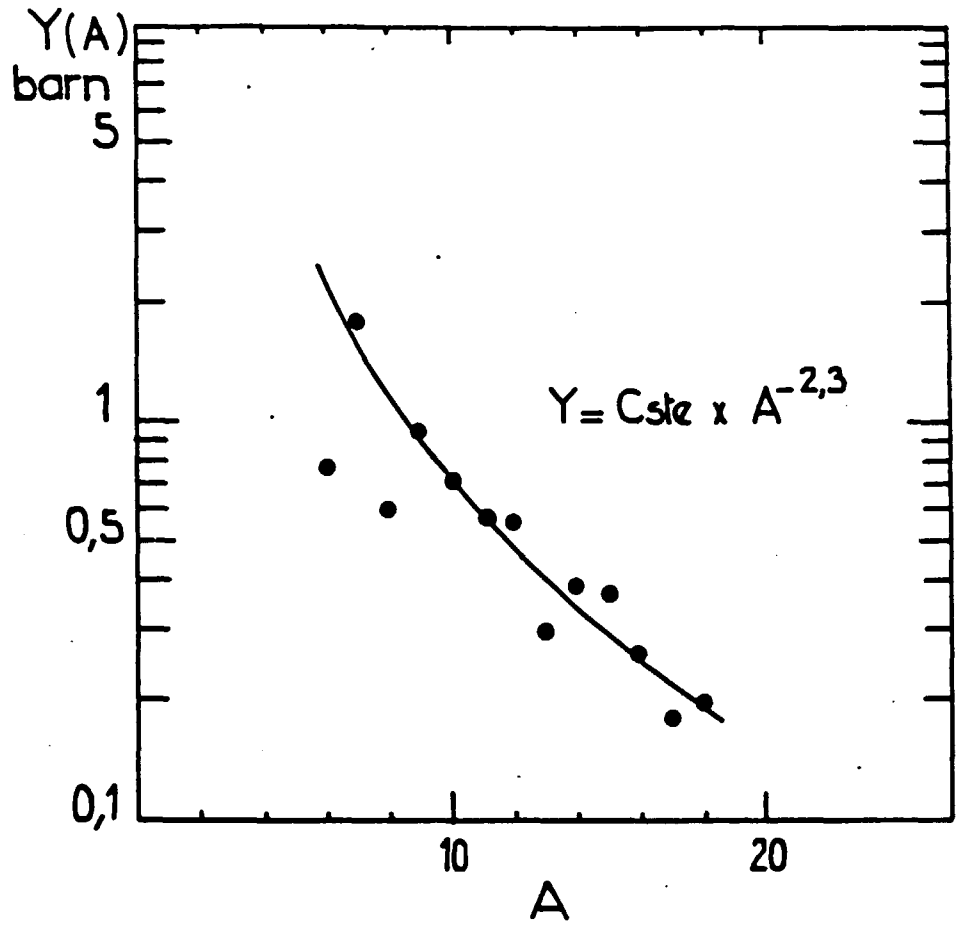

Fig 15

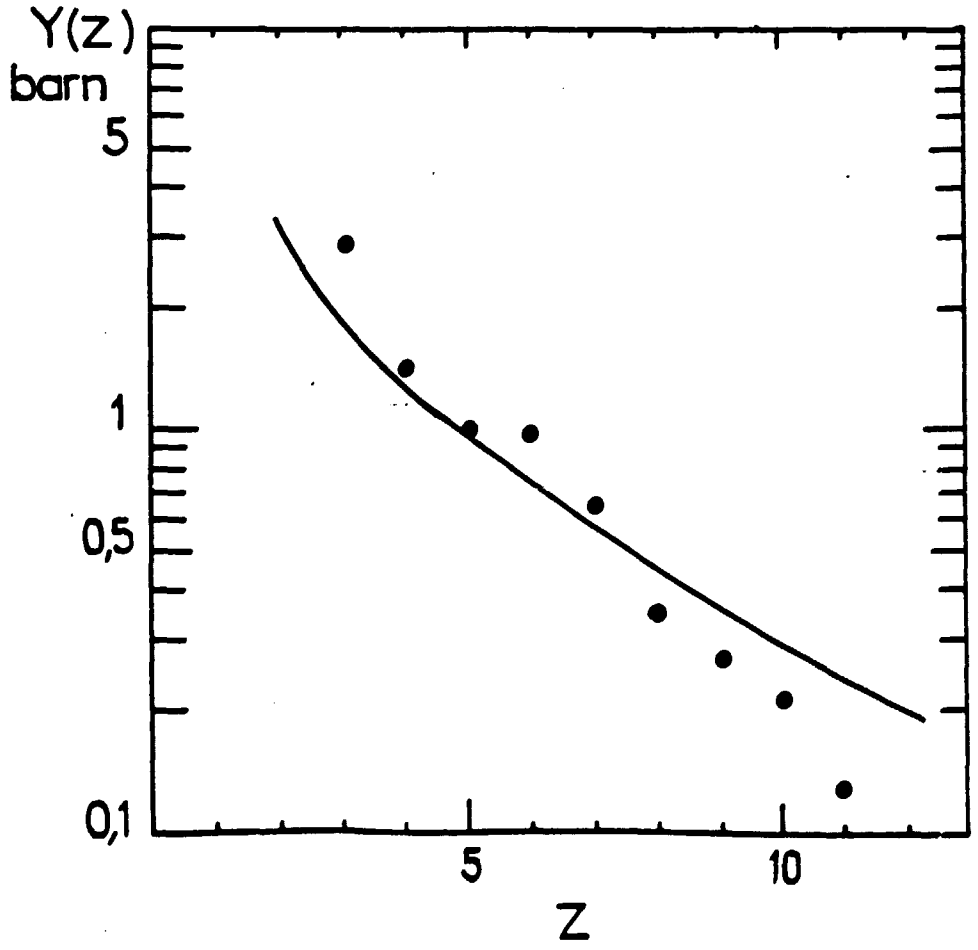

Fig 16